

KEK-PREPRINT-92-65

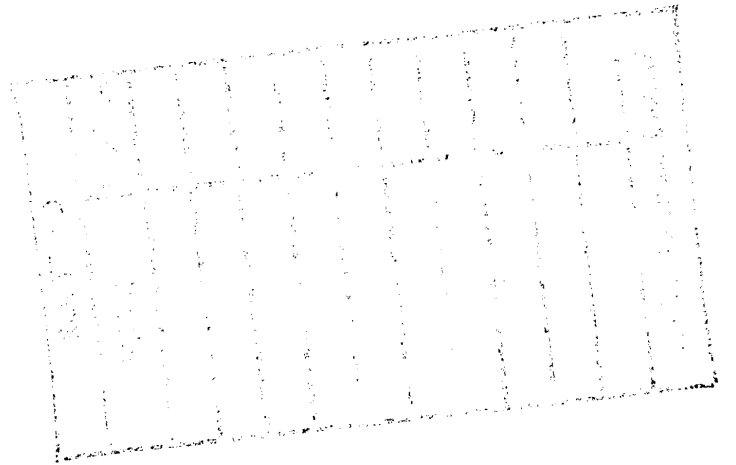


3

KEK Preprint 92-65
July 1992
A

Design of Laser-Compton Spot Size Monitor

T. SHINTAKE, H. HAYANO, A. HAYAKAWA, Y. OZAKI, M. OHASHI,
K. YASUDA, D. WALTZ, S. WAGNER and D. BURKE



*Contributed to the XVth International Conference on High Energy Accelerators,
Congress Centrum, Hamburg, Germany, July 20-24, 1992.*

SEP 1992
FERMILAB

National Laboratory for High Energy Physics, 1992

KEK Reports are available from:

Technical Information & Library
National Laboratory for High Energy Physics
1-1 Oho, Tsukuba-shi
Ibaraki-ken, 305
JAPAN

Phone: 0298-64-1171
Telex: 3652-534 (Domestic)
(0)3652-534 (International)
Fax: 0298-64-4604
Cable: KEKOH

Design of Laser-Compton Spot Size Monitor

T. Shintake and H. Hayano

KEK: National Laboratory for High Energy Physics
1-1 Oho, Tsukuba-shi, Ibaraki-ken, 305 JAPAN

A. Hayakawa, Y. Ozaki, M. Ohashi, and K. Yasuda

KHI: Kawasaki Heavy Industries, Ltd.
1-1 Higashikawasaki-cho 3-chome, Chuo-ku, Kobe 650-91 JAPAN

D. Waltz, S. Wagner and D. Burke

SLAC: Stanford Linear Accelerator Center
Stanford University, Stanford, California, 94305

Abstract

A new diagnostic method for measuring transverse size of electron beam by nondestructive interaction of Compton scattering of laser beam has been proposed⁽¹⁾. A first model of this spot size monitor is under construction for the FFTB - SLAC experiment, in order to measure the electron beam size of 60 nanometer vertical by 1 micrometer horizontal, using Nd: YAG-laser of 1.064 μm wavelength. In this paper, the design of the system, and essential and practical engineering problems are discussed.

1. Introduction

In future e^+e^- linear colliders of TeV region (JLC, VLEPP, NLC, CLIC, ..), the electron and positron beams must be focused into very small spots at the interaction point in order to keep good luminosity. A typical spot size of 100 nm horizontal by a few nm vertical, the flat beam is necessary to get a luminosity near $1 \times 10^{34} \text{ cm}^{-2}\text{s}^{-1}$. This spot size is much smaller than that in any conventional colliding machines, therefore it is one of the most important tasks to develop new technologies of beam diagnostics, especially a reliable spot size measurement system.

In the previous paper^(1,2), a new method was proposed using the standing wave of laser beam. The design work has been started for the first model of this type of monitor, aimed to install at the focus point of the FFTB⁽³⁾ at SLAC. During this design work, several practical problems have been studied and solved. Especially relating to the quality of laser beam, the following points were carefully studied.

- (1) Coherent length of Nd: YAG-laser beam,
- (2) Spatial beam profile,
- (3) Beam pointing stability.

Among them, due to the coherency problem, we have changed the optical arrangement from the intra-cavity scheme to the interferometer scheme. In this scheme, a laser beam is split into two beams of equal intensity by a half mirror, and they are focused again into an identical interaction point with crossing angle. Two laser beams interfere each other, and form the comb shape interference fringe pattern. Since we can make the path length of two beams to be almost equal, the requirement for beam coherency is extensively relaxed.

Additionally, this scheme has a big advantage of the tunability, that is, the spatial pitch of the interference fringes can be varied by choosing the crossing angle of two laser beams, and we can tune the sensitive range of the system for wide range of beam spot size.

2. Principle of Measurement

Figure 2.1 shows the schematic arrangement of the laser Compton spot size monitor. An intense laser beam is split into two beams of equal intensity by a beam splitter, and they are transported along two different arms, and brought into identical cross-focus point: the interaction point. In the interaction point, two traveling waves of laser beam, whose wavefronts are almost plane, overlapping each other with crossing angle of θ , generate comb-shape interference fringes. We inject high energy electron beam into this interference fringes from normal direction of laser beams. Some electrons collide with laser photons, and generates high energy γ -rays by inverse Compton scattering process. We measure the total flux of generated γ -rays pulse-to-pulse using a γ -ray detector located at down stream of the beam line. The electron beam is swept out by a bending magnet located upstream of the γ -ray detector.

When an electron passes through at the bright zone, it will find out more laser photons and generate more γ -rays than in case of passing at the dark zone. Therefore, if we scan the electron trajectory perpendicular to the fringes, the γ -ray flux shows periodic amplitude modulation. Because, the modulation depth depends on the transverse beam size, as shown in Fig. 2.2, from the γ -ray flux measurements we can determine the beam size.

Assuming the laser beam has TEM₀₀-mode, and plane wave fronts at the focus point, the γ -ray flux is given by

$$N = \frac{N_0}{2} [1 + \cos 2k_y \cdot y \cdot \cos \theta \cdot \exp\{-2(k_y \cdot \sigma_y)^2\}] \quad (2.1)$$

where σ_y is the electron bunch size of Gaussian distribution. k_y is the vertical component of the wavenumber: $k_y = k_0 \cdot \sin(\theta/2)$, where $k_0 = 2\pi/\lambda_0$, and θ is crossing angle of two laser beams. From eq. (2.1), the pitch (or period) of the fringe: the distance from a

bright zone to the next bright zones is given by

$$d = \frac{\pi}{k_y} = \frac{\lambda_0}{2 \sin(\theta/2)} \quad (2.2)$$

And, the modulation depth is

$$M = \frac{N_{\max} - N_{\min}}{N_{\max} + N_{\min}} = |\cos\theta| \cdot \exp\{-2(k_y \cdot \sigma_y)^2\} \quad (2.3)$$

It should be noted that even in the case of infinitely small beam ($\sigma_y \rightarrow 0$), the modulation depth does not reach to 100 % due to the term $|\cos\theta|$, this is due to the traveling wave component in the interference fringes, which cause uniform baseline shift in γ -ray modulation curve. Especially, in the special case of normal crossing ($\theta = 90$ degree, $\cos\theta = 0$), the modulation will disappear, therefore we can not use this angle.

From eqs. (2.2) and (2.3), the electron spot size is related to the modulation depth of the γ -ray flux by

$$\sigma_y = \frac{d}{2\pi} \sqrt{2 \cdot \log \frac{|\cos\theta|}{M}} \quad (2.4)$$

The required laser power to get 1000 γ -rays per pulse for a bunch charge of 1×10^{10} electrons is about 10 MW at 1 μm wavelength. This amount of laser power is easily available by commercially provided Q-switch pulsed Nd:YAG-laser system. The detailed discussions on principle of measurement, for the special case of standing wave ($\theta = 180$ deg.) and the calculations of γ -ray flux are given in ref. 1.

3. Design of System

3.1 System overview

Figure 3.1 shows overview of the interferometer system. Every optical components will be mounted on an optical table of 1.8 m by 1.6 m, which is mounted on a dynamically stabilized support table specially designed for the final Q-magnets. The laser system will be located in a clean room outside the accelerator tunnel, and the laser beam will be transported through a vacuum pipe of 20 m distance. At the entrance of the interferometer, position of the laser beam is monitored, its position signal is sent to the laser system, and used for feedback to control a mirror at the exit of the laser oscillator. By this feedback loop, the laser position at the interferometer will be kept within ± 0.5 mm error. In the interferometer, the laser beam is split into six beams, and injected into vacuum interaction chamber through flat windows, and focused at the interaction point. The γ -rays will be measured by a calorimeter located down stream of the beam line.

3.2 Interferometer arrangement

In order to measure the vertical beam size over wide range, and also to measure the horizontal beam size of a few μm range, six laser beam lines will be prepared. By using mechanical shutters, we can select the operating modes as shown in Fig. 3.2. The beam size responses for these modes are plotted in Fig. 3.3. The system has the sensitivity about 1 μm down to 40 nm for vertical, and 4 μm down to 0.7 μm for horizontal.

The special pair mirror after the beam splitter, effects as like a penta prisms, bents the beam direction 90 degree without reversing the image. This is very important to relax the beam alignment tolerance.

3.3 Laser spot size

Because the vertical beta-function β_y^* of electron beam at the final focus point in FFTB is only 100 μm . In order to measure the minimum spot size precisely, we must focus the laser beam into a small spot whose diameter is less than a few times of beta-function. We chose the laser beam spot 200 μm in diameter.

3.4 Damage threshold

In order to prevent the optical components from high power damages, we use long focus lens of f 500 mm. The laser beam sizes on every optical components stay 3 ~ 7 mm in diameter, and power density 0.1 ~ 0.5 GW/cm², which is well below the damage threshold of 5 GW/cm² of dielectric optical coatings on mirrors.

3.5 Longitudinal mode of the laser

In principle, in the interferometer, it is possible to choose the path difference between two laser beams to be zero. However, as shown in Fig. 3.2, in the real system there are path differences order of 5 to 10 cm. The natural width of spectral line of Nd:YAG-laser is about 1 cm⁻¹. Therefore the path difference is longer than the coherent length defined by natural line width of YAG-laser beam, and the interference fringe pattern will be broken.

The required line width to get good interference fringe (visibility > 95%) is 0.01 cm⁻¹. The seeding injection laser technique can reduce the line width of YAG-laser below 0.003 cm⁻¹.

The seeding laser also improves the temporal wave-form of output pulse. The natural waveform of the output power from Q-switched YAG-laser shows high frequency spikes. This is due to overlapping of many longitudinal modes inside the laser resonator. The seeding laser scheme limits the longitudinal mode to a single mode, and makes the temporal profile to a smooth waveform (Fourier limited waveform). Therefore, the timing jitter of 1 nsec from Q-switch trigger to the light pulse does not cause substantial intensity fluctuations at the beam timing, where the half width of pulse is about 9 nsec.

3.6 Laser beam transport system

In order to prevent the laser system from radiation damage and also to easily access for maintenance, the laser system will be installed in a clean room outside the linac tunnel, and the laser beam will be transported through a vacuum pipe for 20 m distance. The clean room and laser transport system is under construction at SLAC.

3.7 High resolution BPM

In order to measure the electron beam position at the interaction point precisely, a new type beam position monitor using TM₁₁₀-mode resonance in pill-box cavity will be installed. This monitor, in principle, has very high spatial resolution, better than 10 nm for 1 nC bunch charge. Cold test cavity is under fabrication.

4. Conclusions

The system is under construction. We will complete the construction of the system until the next spring, and start the beam test in FFTB at April 1993. In the future linear collider, this system will be installed

at the collision point, and utilized for measurement of beam size of nm range in order to tune the final focus beam line.

References

- (1) Tsumoru SHINTAKE, "Proposal of a nanometer beam size monitor for e^+e^- linear colliders", Nucl. Instrum. and Meth. in Physics Research A311 (1992) 453 - 464.
- (2) Tsumoru SHINTAKE, "Nano-meter Beam Size Monitor by Laser-Compton Scattering", proceedings of the 8th symp. on Accelerator Science and Technology, Nov. 25-27, 1991, Saitama, Japan, pp. 290 - 292.
- (3) "Final Focus Test Beam, project design report", SLAC-Report-376, UC-414 (A/I) March 1991.

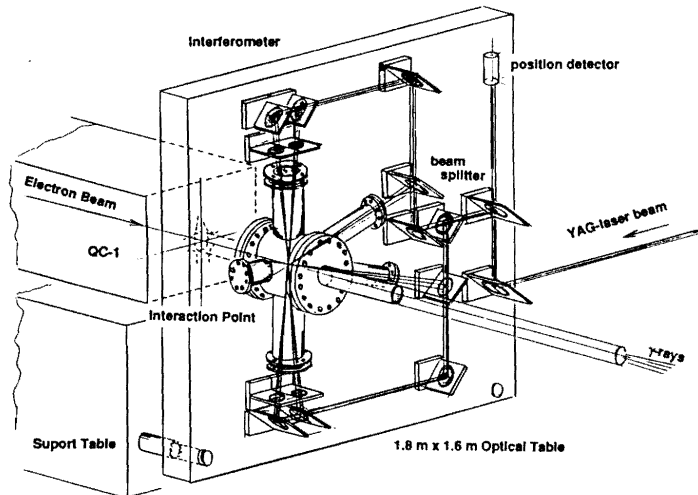


Fig. 3.1 Overview of beam size monitor system. (interferometer block)

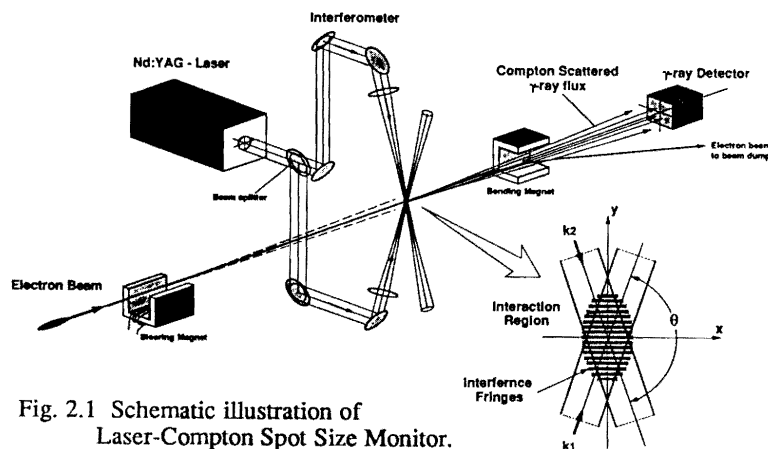


Fig. 2.1 Schematic illustration of Laser-Compton Spot Size Monitor.

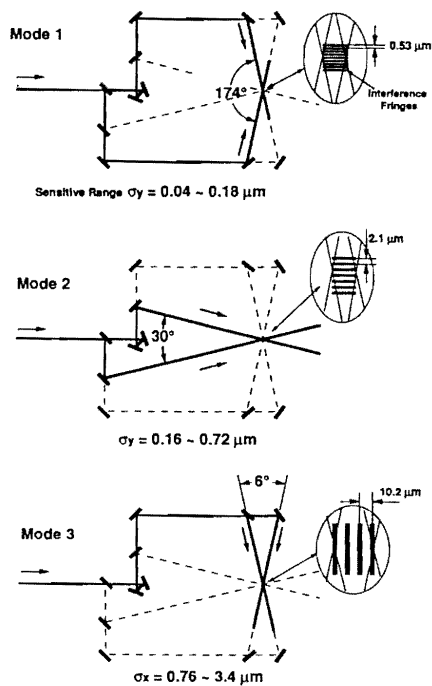


Fig. 3.2 Operation modes.

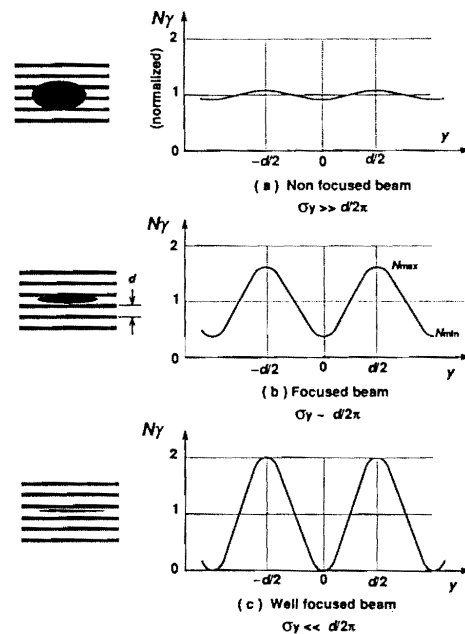


Fig. 2.2 γ -ray flux modulation pattern.

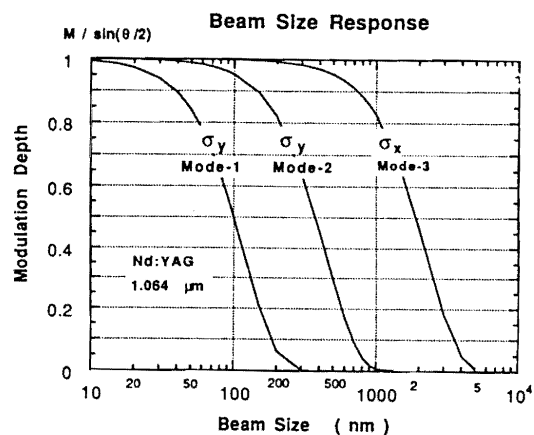


Fig. 3.3 Beam size response curves.